Macrodimers: Ultralong Range Rydberg Molecules

Christophe Boisseau, Ionel Simbotin, and Robin Côté*
Physics Department, University of Connecticut, 2152 Hillside Road, Storrs, Connecticut 06269-3046
(Received 3 August 2001; published 19 March 2002)

We study long range interactions between two Rydberg atoms and predict the existence of ultralong range Rydberg dimers with equilibrium distances of many thousands of Bohr radii. We calculate the dispersion coefficients C_5, C_6, and C_8 for two rubidium atoms in the same excited level np and find that they scale like n^8, n^{11}, and n^{15}, respectively. We show that for certain molecular symmetries these coefficients lead to long range potential wells that can support molecular bound levels. Such macrodimers would be very sensitive to their environment and could probe weak interactions. We suggest experiments to detect these macrodimers.

DOI: 10.1103/PhysRevLett.88.133004 PACS numbers: 32.80.Rm, 32.80.Pj, 34.20.Cf

New techniques used for cooling and trapping of atoms [1] and molecules [2], and which led to the realization of atomic Bose-Einstein condensation [3], have also been applied to experiments with ultracold plasmas [4] and ultracold Rydberg atoms [5]. The exaggerated properties of Rydberg atoms provide a fertile ground for new physics. For example, transport properties of ultracold gases doped with ions were recently explored and extended to cold Rydberg samples [6], while entangled states relevant for quantum computing can also be produced with ultracold Rydberg atoms [7]. Finally, the creation of "trilobite" Rydberg molecules was proposed [8], where one atom of the dimer remains in its ground state while the second one is excited to a Rydberg state.

In this Letter, we explore the interactions between two Rydberg atoms. We show that long range wells supporting several bound levels exist for certain molecular symmetries. We explore the sensitivity of these wells to the particular asymptotic form of the potential long range expansion and show that their existence is robust. We also estimate the effect of retardation as well as the validity of the Born-Oppenheimer approximation. We give numerical examples for the case of rubidium (Rb) and discuss experimental schemes to detect these macrodimers. These molecules could lead to measurements of very weak interactions, such as vacuum fluctuations, and provide a unique tool to study quenching in ultracold collisions.

We consider two atoms each excited by one photon from their ground state into the same Rydberg state np [9], where n is the principal quantum number. For Rb, this corresponds to the $5s \rightarrow np$ transition [10]. At large separation R, the potential energy between two atoms can be expanded in powers of $1/R$ [11]. For two identical atoms in the same np state, it takes the form [12]

$$V(R) = -\frac{C_5}{R^5} - \frac{C_6}{R^6} - \frac{C_8}{R^8}, \quad (1)$$

where the dispersion coefficients C_5, C_6, and C_8 depend on n. For the $np - np$ asymptote of the homonuclear dimers, we have in total six pairs of degenerate molecular states with identical coefficients for each pair: $^1\Delta_g$ and $^3\Delta_u$, $^1\Pi_g$ and $^3\Pi_u$, $^3\Pi_g$ and $^1\Pi_u$, $^3\Sigma_g^-$ and $^1\Sigma_u^-$, and two pairs of $^1\Sigma_g^+$ and $^3\Sigma_u^+$ [12]. Note that the degeneracy of any pair of molecular states is lifted by the exponentially decaying exchange interactions, which can be neglected at large enough R.

The numerical values of C_5, C_6, and C_8 [13] were calculated using the expressions of Marinescu [12]. The sums over the electronic states were evaluated directly, and using the n scaling of the dipole ($\propto n^2$), quadrupole ($\propto n^4$), and octopole ($\propto n^6$) matrix elements and the energy differences ($\propto n^{-3}$) involved, we obtained the following scaling laws: $C_5 \propto n^8$, $C_6 \propto n^{11}$, and $C_8 \propto n^{15}$. The magnitude and sign of the dispersion coefficients depend on the molecular symmetry considered, and it is possible to obtain a long range potential well with an attractive long range R^{-5} contribution and a repulsive shorter range R^{-6} or R^{-8} contribution (see Fig. 1). For the $np - np$ asymptote, we found that three pairs of degenerate molecular states give long range potential wells: $^1\Pi_g$-$^3\Pi_u$, $^3\Sigma_g^-$-$^1\Sigma_u^-$, and one of $^1\Sigma_g^+$-$^3\Sigma_u^+$.

For the system to be adequately described by Eq. (1), the exchange energy must be negligible. To estimate the region of validity of Eq. (1), we use the Le Roy radius $R_{\rm LR}$ [14] as a measure of the electron wave function overlap between the two atoms: it is given by $R_{\rm LR} = 2(\langle r^2\rangle_A^{1/2} + \langle r^2\rangle_B^{1/2})$, where $\langle r^2\rangle_{A,B}^{1/2}$ is the rms position of the electron

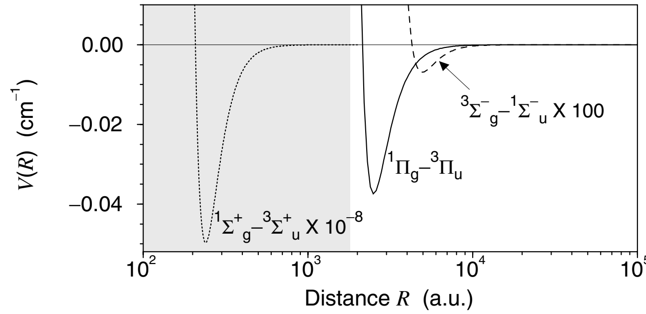

FIG. 1. Comparison of the potential curves for the three pairs of states that sustain a well for Rb ($n = 20$). Inside the shaded area we have $R < R_{\rm LR}$, and Eq. (1) is not adequate.

 0031-9007/02/88(13)/133004(4)$20.00

of atom A (B) [15]. If $R < R_{\mathrm{LR}}$, exchange and charge-overlap interactions become important and Eq. (1) is not adequate to describe the system.

In Fig. 1, we illustrate the wells for the three pairs of degenerate states $^1\Pi_g$-$^3\Pi_u$, $^3\Sigma_g^-$-$^1\Sigma_u^-$, and $^1\Sigma_g^+$-$^3\Sigma_u^+$ of Rb with $n = 20$. The Le Roy radius R_{LR} is equal to $1902a_0$, where a_0 is a Bohr radius. The well of the pair of states $^1\Sigma_g^+$-$^3\Sigma_u^+$ is very deep (potential depth $D_e = 4.5 \times 10^6$ cm^{-1}) but is located at a much shorter distance than the Le Roy radius (equilibrium distance $R_e = 240a_0$): the interactions for these states are not well described by Eq. (1), as opposed to the two other pairs. The well of the pair $^1\Pi_g$-$^3\Pi_u$ has a depth $D_e = 3.74 \times 10^{-2}$ cm^{-1} and an equilibrium distance $R_e = 2509a_0$. By comparison, the well of the pair $^3\Sigma_g^-$-$^1\Sigma_u^-$ is much shallower and farther away, with $D_e = 6.88 \times 10^{-5}$ cm^{-1} and $R_e = 4956a_0$. In Fig. 2, we compare D_e, R_e, and R_{LR} for the three pairs for various values of n and find the same general behavior. For the remainder of this Letter, we focus our attention on the deeper wells described by Eq. (1), i.e., the $^1\Pi_g$-$^3\Pi_u$ pair, since the much shallower wells of the $^3\Sigma_g^-$-$^1\Sigma_u^-$ pair may prove more difficult to detect.

In Fig. 3, we illustrate the scaling of the dispersion coefficients, equilibrium distance, and well depth of the $^1\Pi_g$-$^3\Pi_u$ pair as a function of n. In atomic units, the coefficients are given approximately by $C_5 \sim 3n^8$, $C_6 \sim -0.7n^{11}$, and $C_8 \sim -50n^{15}$ [see Fig. 3(a)]. Neglecting C_8 in Eq. (1) and setting the derivative of $V(R)$ to zero, we find that the equilibrium distance scales as $R_e \sim 0.3n^3a_0$, in good agreement with the numerical values shown in Fig. 3(b). The scaling of D_e is 10^8n^{-7} cm^{-1}, as expected [see Fig. 3(b)]. Note that other pairs may have different R_e and D_e scaling, depending on the relative magnitude of the dispersion terms. The wells for the $^1\Pi_g$-$^3\Pi_u$ pair, although shallow, support many vibrational bound levels. In Table I, we list the two lowest and highest levels found for $n = 20$, 40, and 70 [16], which support 143, 125, and 107 bound levels, respectively. While the wells for high n are much shallower than those with smaller n (e.g., see $n = 20$ and 70 in Table I), their larger extension leads to denser energy levels, and hence they also support a large number of levels.

When using the expression for $V(R)$, the Born-Oppenheimer approximation is assumed valid. To verify that it is the case, we compare the vibrational period $\tau_{\mathrm{vib}}(v)$ of a given bound level v with the typical time for the electron motion $\tau_e = h/|E_n| = (4\pi/\alpha c)n^2a_0$, where E_n is the electron binding energy. If $\tau_e/\tau_{\mathrm{vib}} \ll 1$, the Rydberg electrons of both atoms easily follow the motion of the ions, and the Born-Oppenheimer curve $V(R)$ needs no further diabatic corrections. Taking the levels in Table I as examples, for $n = 20$, we find $\tau_e/\tau_{\mathrm{vib}} \sim 1.5 \times 10^{-6}$ for the lowest level $v = 0$, and 2.2×10^{-11} for the highest level $v = 142$: the electrons follow adiabatically the ions for all vibrational levels. For $n = 70$, the ratio becomes 6.8×10^{-9} for $v = 0$ and 4.5×10^{-14} for $v = 106$. Naturally, the Born-Oppenheimer approximation gets better for the higher vibrational levels, since they are more extended and therefore take more time to make a full oscillation. However, the spontaneous decay of one of the excited Rydberg atoms will limit the lifetime of these long range molecules and prevent the existence of the upper lying vibrational bound levels. Although the lifetime of the excited atoms is long, scaling as $\tau_{\mathrm{at}} \sim \tau_0 n^3$, where $\tau_0 \sim 1.4$ ns [17], it is much shorter than the vibrational period for high v. For example, for $n = 20$, we find $\tau_{\mathrm{at}} \sim 11.2$ μs and $\tau_{\mathrm{vib}} = 0.083$ μs and 5.58 ms for $v = 0$ and 142, respectively, and for $n = 70$, $\tau_{\mathrm{at}} \sim 480$ μs and $\tau_{\mathrm{vib}} = 220$ μs and 32.8 s for $v = 0$ and 106, respectively. In effect, the upper vibrational levels can be

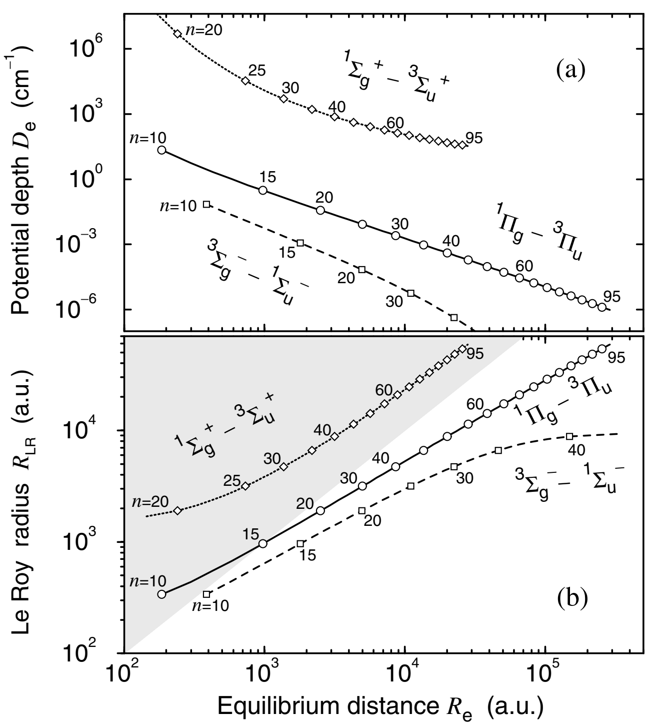

FIG. 2. In (a), comparison of D_e as a function of R_e for the three pairs supporting long range wells, for various n. In (b), R_e is compared to R_{LR} for the same states. The shaded area is defined by $R_e < R_{\mathrm{LR}}$.

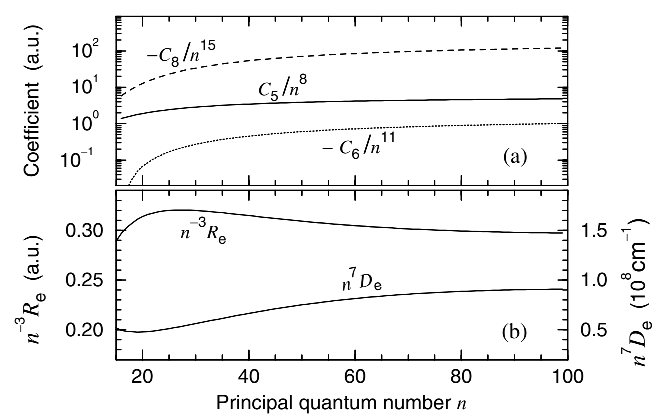

FIG. 3. Scaling of (a) C_5, C_6, C_8 for the $^1\Pi_g$-$^3\Pi_u$ pair and (b) R_e (left scale) and D_e (right scale), as a function of n.

TABLE I. Sample of vibrational bound levels for the ${}^1\Pi_g$-${}^3\Pi_u$ pair. The top corresponds to $n = 20$, with $R_e = 2509a_0$, $D_e = 3.740 \times 10^{-2}$ cm^{-1}, the middle to $n = 40$, with $R_e = 20\,141a_0$, $D_e = 4.060 \times 10^{-4}$ cm^{-1}, and the bottom to $n = 70$, with $R_e = 103\,380a_0$, $D_e = 1.042 \times 10^{-5}$ cm^{-1}.

v	E_b (cm^{-1})	$E(v)$ (cm^{-1})	R_1 (a_0)	R_2 (a_0)	$\tau_{\rm vib}$ (s)
0	−3.70 [−2]	4.01 [−4]	2454	2571	8.3 [−8]
1	−3.62 [−2]	1.19 [−3]	2417	2623	8.4 [−8]
⋮					
141	−3.46 [−8]	3.74 [−2]	2142	49 859	1.2 [−3]
142	−3.89 [−9]	3.74 [−2]	2142	77 220	5.6 [−3]
0	−4.01 [−4]	5.04 [−6]	19 651	20 701	6.6 [−6]
1	−3.91 [−4]	1.50 [−5]	19 331	21 163	6.7 [−6]
⋮					
123	−3.27 [−10]	4.06 [−4]	17 111	431 262	0.1
124	−1.91 [−11]	4.06 [−4]	17 111	762 169	0.8
0	−1.03 [−5]	1.52 [−7]	100 574	106 629	2.2 [−4]
1	−9.97 [−6]	4.51 [−7]	98 762	109 334	2.3 [−4]
⋮					
105	−1.02 [−11]	1.04 [−5]	87 306	2 211 658	3.1
106	−3.57 [−13]	1.04 [−5]	87 306	4 337 482	32.8

considered as quasicontinuum states since only a fraction of an entire oscillation will take place before deexcitation.

Another effect limiting the existence of Rydberg long range molecules is autoionization. When two excited atoms interact, one atom can decay to a lower excited state while the second atom is ionized, the free electron picking up most of the kinetic energy. However, if the separation between the Rydberg atoms is larger than $R_{\rm LR}$, there is little overlap between their electronic clouds, and one expects the autoionization probability to be small (the atoms interact via their electric dipoles at such distances). Note also that for alkali dimers in general [18], and Rb in particular, avoided crossings with the ionic curves (here correlated to $\mathrm{Rb}^+ + \mathrm{Rb}^-$) perturb the lowest asymptotes such as $5p - 5p$. However, for the case where the Le Roy radius condition is satisfied, i.e., for $n \geq 20$ [see Fig. 2(b)], the $np - np$ asymptotes are much higher than the ionic curves, and no perturbation from avoided crossings will occur.

The density of electronic states in the Rydberg region is very large, and avoided crossings from potential curves correlated to other asymptotes with the same symmetry could perturb the shallow wells. However, the closest asymptotes are generally separated by several times the potential depth D_e, and no avoided crossing in the well region occurs [19]. Figure 4 illustrates the well for $40p - 40p$ and the two nearest curves correlated to $36s - 47p$ and $42s - 36f$, for the ${}^1\Pi_g$-${}^3\Pi_u$ symmetries. The separation between them is much larger than D_e and no crossings occur. Although the various asymptotes become denser as n increases, the potentials become very shallow ($D_e \propto n^{-7}$), and generally no crossing is found. Note that avoided crossings from a lower asymptote repulsive curve and a higher asymptote attractive curve (with the same symmetry) could, in fact, produce deep wells.

For these extremely extended states, retardation effects may become important. Again, to estimate the importance of the photon time of flight, we compare the electronic time τ_e with the time it takes a photon to cover the distance between the two centers: $\tau_{\rm ph} \sim R/c$. For the highest levels, the relevant distance is the outer turning point R_2, but for the deeper levels, a good estimate is obtained by using the equilibrium distance R_e. Using the scaling $R_e \sim 0.3n^3$, we have $\tau_{\rm ph}/\tau_e \sim (0.3\alpha/4\pi)n \ll 1$ for $n < 100$. For the highest vibrational levels v in Table I, we get $\tau_{\rm ph}/\tau_e \sim 0.07$ and 0.11, for R_2 of $v = 141$ and 142, respectively (for $n = 20$), and $\tau_{\rm ph}/\tau_e \sim 0.26$ and 0.51 for R_2 of $v = 105$ and 106, respectively (for $n = 70$). Although retardation effects are not important for the lower vibrational

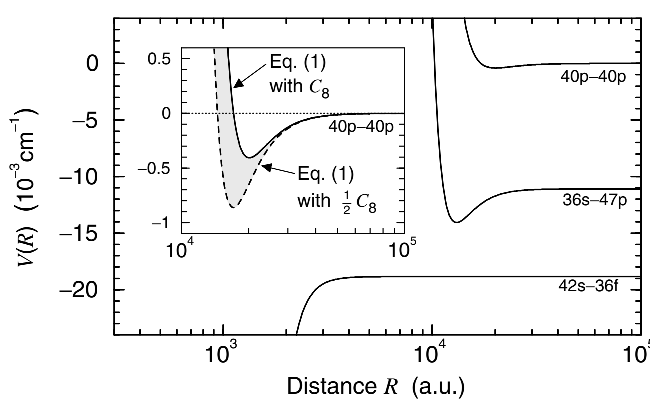

FIG. 4. Nearest asymptotes to $40p - 40p$ for the ${}^1\Pi_g$-${}^3\Pi_u$ symmetries. Inset: convergence of Eq. (1) for $n = 40$. The shaded area gives an estimate of the truncation error.

levels (with R_2 slightly larger than R_e), even for large n, one needs to consider them for the higher vibrational levels. The sensitivity of the interaction potential to retardation effects could actually be used to detect these effects using high precision spectroscopy.

We included three terms in the asymptotic $1/R$ expansion (1), but one has to verify the effect of the truncation on the well properties. The standard procedure to estimate the maximum error due to the truncation of higher terms is to include half of the last term [20]: here, C_8. In Fig. 4, we illustrate the effect of such a variation for $n = 40$. The well becomes deeper but is still located outside the Le Roy radius; hence the existence of long range wells is robust to the truncation of the $1/R$ expansion.

To detect these Rydberg macrodimers, one could photoassociate them from the ground state ($5s$ for Rb) to the target molecular symmetry. After the photoassociation pulse [10], one can field ionize the system and detect the ions. The existence of the molecules should lead to small peaks red-detuned from the atomic asymptote. Because the spacing of the bound levels is small, individual levels will be hard to detect (a laser width smaller than the spacing Δ is needed: for $n = 20$, $\Delta \sim 10^{-3}$ cm^{-1} ~ 300 MHz for the deepest levels), and the most probable signature would be an overall red-detuned peak. The wells are shallow, and only those deep enough could be detected. To enhance the sensitivity of the detection scheme, one could also use radio frequency to excite a bound level to a continuum state corresponding to another asymptote [e.g., to $(n + 1)s - np$]. The detection of any $(n + 1)s$ atoms (e.g., by ramp-field ionization) would be attributed to the existence of a long range bound molecular state, since the rf field would not be resonant with free np atoms.

We have computed long range interactions between two Rb atoms in the same np state and found that shallow long range wells supporting several vibrational levels exist for certain molecular symmetries. Although specific calculations were performed for Rb and $np - np$ asymptotes, the existence of these macrodimers is general: one can expect them for various asymptotes $n_1\ell_1 - n_2\ell_2$ and for all alkali atoms. Furthermore, avoided crossing between curves of the same symmetry with different asymptotes could also provide deep long range molecular wells, in a manner similar to the long range wells observed in many alkali dimers [21]. The macrodimers are extremely sensitive to their environment, and as such, they could be used as probes for extremely weak interactions, e.g., to measure retardation effects and vacuum fluctuations, or any weak electromagnetic interaction. Also, due to their very small rovibrational energy splittings, macrodimers would provide a unique tool to study quenching in ultracold collisions, since they would remain trapped (as opposed to usual dimers [22]). Finally, the detection of such exotic molecules in itself would be a considerable achievement.

The authors thank A. Dalgarno, V. Kharchenko, P. L. Gould, and E. Eyler for helpful discussions. This work was supported by the University of Connecticut Research Foundation, the Research Corporation, and Grant No. ITR-0082913 from the National Science Foundation.

*Electronic address: rcote@phys.uconn.edu

[1] J. Weiner *et al.,* Rev. Mod. Phys. **71**, 1 (1999).
[2] A. Fioretti *et al.,* Phys. Rev. Lett. **80**, 4402 (1998); T. Takekoshi, B. M. Patterson, and R. J. Knize, Phys. Rev. Lett. **81**, 5105 (1998); A. N. Nikolov *et al.,* Phys. Rev. Lett. **82**, 703 (1999); W. C. Stwalley and H. Wang, J. Mol. Spectrosc. **195**, 236 (1999); R. Côté *et al.,* Phys. Rev. Lett. **74**, 3581 (1995).
[3] K. B. Davis *et al.,* Phys. Rev. Lett. **75**, 3969 (1995); M. H. Anderson *et al.,* Science **269**, 198 (1995); C. C. Bradley *et al.,* Phys. Rev. Lett. **75**, 1687 (1995); D. G. Fried *et al.,* Phys. Rev. Lett. **81**, 3811 (1998).
[4] T. C. Killian *et al.,* Phys. Rev. Lett. **83**, 4776 (1999).
[5] W. R. Anderson, J. R. Veale, and T. F. Gallagher, Phys. Rev. Lett. **80**, 249 (1998); I. Mourachko *et al., ibid.* **80**, 253 (1998).
[6] R. Côté and A. Dalgarno, Phys. Rev. A **62**, 012709 (2000); R. Côté, Phys. Rev. Lett. **85**, 5316 (2000).
[7] D. Jaksch *et al.,* Phys. Rev. Lett. **85**, 2208 (2000); M. D. Lukin *et al.,* Phys. Rev. Lett. **87**, 037901 (2001).
[8] C. H. Greene, A. S. Dickinson, and H. R. Sadeghpour, Phys. Rev. Lett. **85**, 2458 (2000).
[9] Other cases with $np + n'p$, $ns + n's$, or $ns + n'd$ could be explored. See M. Marinescu and A. Dalgarno, Phys. Rev. A **52**, 311 (1995); M. Marinescu and H. R. Sadeghpour, Phys. Rev. A **59**, 390 (1999).
[10] A short intense laser pulse (e.g., 10 MW/cm^2 during 10 ns) photoassociates all atom pairs with the right separation. The number of macrodimers produced will depend only on the pairs' spatial distribution.
[11] A. Dalgarno and W. D. Davison, Adv. Mol. Phys. **2**, 1 (1966).
[12] M. Marinescu, Phys. Rev. A **56**, 4764 (1997).
[13] The dipole, quadrupole, and octupole radial matrix elements were obtained using the quantum defect of $p_{1/2}$ to evaluate electronic wave functions. See [17].
[14] R. J. Le Roy, Can. J. Phys. **52**, 246 (1974).
[15] A modified definition can be found in B. Ji, C.-C. Tsai, and W. C. Stwalley, Chem. Phys. Lett. **236**, 242 (1995).
[16] Special attention near the dissociation limit was necessary to obtain the bound levels. See C. Boisseau *et al.,* Eur. Phys. Lett. **12**, 199 (2000).
[17] T. F. Gallagher, *Rydberg Atoms* (Cambridge University Press, Cambridge, 1994).
[18] S. Magnier *et al.,* J. Phys. B **27**, 1723 (1994).
[19] For rare accidental near degeneracies where other asymptotes are close compared to D_e, one needs to diagonalize the appropriate interaction subspace.
[20] A. Dalgarno and J. T. Lewis, Proc. Phys. Soc. A **69**, 57 (1956).
[21] W. C. Stwalley, Y.-H. Uang, and G. Pichler, Phys. Rev. Lett. **41**, 1164 (1978); H. Wang, P. L. Gould, and W. C. Stwalley, Z. Phys. D **35**, 317 (1996).
[22] R. C. Forrey *et al.,* Phys. Rev. A **59**, 2146 (1999).